

Critical comparison of classical field theory and microscopic wave functions for skyrmions in quantum Hall ferromagnets

M. Abolfath*

Department of Physics, Indiana University, Bloomington, Indiana 47405

J. J. Palacios

*Department of Physics, Indiana University, Bloomington, Indiana 47405
and Department of Physics and Astronomy, University of Kentucky, Lexington, Kentucky 40506*

H. A. Fertig

Department of Physics and Astronomy, University of Kentucky, Lexington, Kentucky 40506

S. M. Girvin and A. H. MacDonald

Department of Physics, Indiana University, Bloomington, Indiana 47405

(Received 14 May 1997)

We report on a study of the classical field theory description of charged skyrmions in quantum Hall ferromagnets. The appropriate field theory is a nonlinear σ model generalized to include Coulomb and Zeeman interaction terms. We have tested the range of validity of the classical field theory by comparing with microscopic descriptions of the single-skyrmion state based on the Hartree-Fock approximation, exact diagonalization calculations, and many-body trial wave functions. We find that the field theory description is accurate for skyrmions with moderate spin quantum numbers (≥ 10) although, as expected, it fails qualitatively for small spin quantum numbers. [S0163-1829(97)02935-4]

I. INTRODUCTION

The quantum Hall effect¹⁻⁴ occurs in a two-dimensional electron system (2DES) in a strong perpendicular magnetic field (B) and is associated with the existence of incompressible ground states at certain values of the Landau level filling factor ν . ($\nu \equiv N/N_\phi$ where N_ϕ is the Landau level degeneracy and N is the number of electrons in the system.) Some incompressible ground states are strong ferromagnets, i.e., they are total spin eigenstates with $S = N/2$ so that an infinitesimal Zeeman coupling of the magnetic field to the spin degree of freedom is sufficient to produce complete spin alignment. Because of the small ratio of the Zeeman splitting to other relevant energy scales in typical 2DES's, it is then useful to regard the system as a ferromagnet in a weak symmetry breaking magnetic field, even though the 2DES is often in the strong field quantum limit as far as orbital degrees of freedom are concerned. Quantum Hall ferromagnets (QHF's) have a number of unusual properties that spring from the disparity between the magnetic field coupling strengths for orbital and spin degrees of freedom.

Because of the gap for charged excitations in incompressible states, the only low-lying excitations in these quantum Hall ferromagnets are those associated with slow variations in the unit vector field which describes the local orientation of the spin magnetic moment. In addition to the spin wave modes, there exist higher-energy topologically nontrivial skyrmion^{5,6} textures in the spin field. The importance of these topologically nontrivial excitations is magnified by the fact that they carry an electrical charge.^{6,7} As the lowest-energy charge carriers they control the thermally activated dissipation on the $\nu=1$ quantum Hall plateau and, away

from filling factor $\nu=1$, they are present in the ground state.⁸⁻¹⁰ In the latter case the ground state is no longer fully spin polarized. For weak Zeeman coupling skyrmions are large and each charge introduced into the system flips over a large number of spins. Thus the spin magnetization is expected to show a sharp cusp at filling factor $\nu=1$.

The presence of these objects has recently been detected directly in NMR measurements of the electron spin magnetization which is proportional to the Knight shift,¹¹ in thermal transport measurements,¹² and in optical absorption.¹³ They may also be responsible for the recently observed¹⁴ enormous enhancement of the apparent specific heat because of their equilibrating effect on the nuclear spins. There has recently been considerable interest in the physics of these exotic electronic quasiparticles.^{5-10,15-25}

Charged spin texture excitations in QHF's are the subject of this paper. A realistic theory of these excitations requires at a minimum that Coulomb energy and Zeeman energy terms be added to the nonlinear sigma ($NL\sigma$) model classical field theory. In Sec. II we briefly review the resulting classical field theory of spin textures in QHF's and report on numerical solutions for the lowest-energy topologically nontrivial textures. With typical parameters, the size of the lowest-energy textures need not be large compared to microscopic lengths so that both higher-order gradient corrections and quantum fluctuations not included in the model may become important. In Sec. III we present an overview of the various microscopic approaches which have been used to study skyrmion states in quantum Hall ferromagnets. In the Hartree-Fock approximation, the gradient expansion of the field theory is effectively summed to infinite order. However, it becomes difficult to solve these equations accurately for

very large skyrmions. Many-particle variational wave function and exact diagonalization approaches also incorporate, in addition, quantum fluctuation effects, but are even more limited in the size of quasiparticles for which accurate calculations are possible. Numerical comparisons of energies and spin densities obtained using these different approximation strategies are compared in Sec. IV. One conclusion from this work is that the most important corrections to the minimal generalized NL σ model are the higher-order gradient corrections already captured in the Hartree-Fock approximation. The quantum fluctuations added using trial wave function or exact diagonalization are responsible only for minor further modifications. We summarize our conclusions in Sec. V.

II. CLASSICAL FIELD THEORY

A. General considerations

Here we briefly review the classical field theory for charged spin texture excitations or skyrmions in quantum Hall ferromagnets.^{6,7} Following Sondhi *et al.*,⁶ we start from a modified version of the NL σ model classical field theory which has been exploited to describe the low-energy properties of two-dimensional Heisenberg ferromagnets and antiferromagnets.^{26–29} The order parameter in this theory is a unit vector field, $\mathbf{m}(\mathbf{r})$, that describes the local orientation of the spin or pseudospin⁷ magnetic order. For quantum Hall ferromagnets the energy functional of the minimal theory is

$$E[\mathbf{m}] = E_0[\mathbf{m}] + E_z[\mathbf{m}] + E_c[\mathbf{m}], \quad (1)$$

where $E_0[\mathbf{m}]$ is the leading-order term in a gradient expansion of the energy functional and $E_z[\mathbf{m}]$ is the Zeeman energy functional:

$$E_0[\mathbf{m}] = \frac{\rho_s}{2} \int d^2r (\nabla \mathbf{m})^2, \quad (2a)$$

$$E_z[\mathbf{m}] = \frac{t}{2\pi\ell_0^2} \int d^2r [1 - m_z(\mathbf{r})]. \quad (2b)$$

Here $\rho_s = e^2/(16\sqrt{2}\pi\epsilon\ell_0)$ is the spin stiffness [assuming zero layer thickness for the two-dimensional electron gas (2DEG)] which can be calculated analytically for this case and represents a loss of Coulomb exchange energy, $t = (g^* \mu_B B)/2$ represents the Zeeman coupling strength, ϵ is the dielectric constant of the host semiconductor, and ℓ_0 is the magnetic length.

When only these first two terms are present, the spatial extent of structure in skyrmion extrema of the energy functional shrinks to a point and the gradient expansion fails. To obtain a consistent theory of skyrmion excitations when the Zeeman coupling is nonzero it is necessary to go beyond leading order in the gradient expansion. For QHF's it turns out⁶ that, because skyrmions are charged, the next to leading term in the gradient expansion is the nonlocal Coulomb interaction energy functional

$$E_c[\mathbf{m}] = \frac{e^2}{2\epsilon} \int d^2r \int d^2r' \frac{\rho(\mathbf{r})\rho(\mathbf{r}')}{|\mathbf{r} - \mathbf{r}'|}, \quad (2c)$$

where the charge density is given by^{6,7}

$$\rho(\mathbf{r}) = \frac{-\nu}{8\pi} \epsilon_{ab} \mathbf{m}(\mathbf{r}) \cdot [\partial_a \mathbf{m}(\mathbf{r}) \wedge \partial_b \mathbf{m}(\mathbf{r})]. \quad (3)$$

The charge density is the product of the Landau level filling factor of the ground state ν and the $O(3)$ topological density of the spin texture. The nonlocality of this functional complicates the calculations we present below. The total skyrmion charge is therefore ν times an integer-valued topological invariant. If we compact the 2D plane to a sphere S^2 , then $\mathbf{m}(\mathbf{r})$ defines a mapping of S^2 onto the order parameter sphere S^2 and hence can be classified by the homotopy group $\pi_2(S^2)$. The topological charge simply counts the wrapping of the order parameter sphere by the coordinate sphere.^{30,31}

Extrema of the energy functional of this model, $\tilde{\mathbf{m}}$, satisfy a nonlinear differential equation which can be obtained by minimizing Eq. (1) with respect to \mathbf{m} , using a Lagrange multiplier to enforce the constraint $\mathbf{m}(\mathbf{r}) \cdot \mathbf{m}(\mathbf{r}) = 1$. After eliminating the Lagrange multiplier we find that

$$\rho_s (-\nabla^2 + \tilde{\mathbf{m}} \cdot \nabla^2 \tilde{\mathbf{m}}) \tilde{m}_\mu - \frac{t}{2\pi\ell_0} (\delta_{z\mu} - \tilde{m}_z \tilde{m}_\mu) - \frac{\nu}{4\pi} \epsilon_{ab} \{\partial_a V(\mathbf{r})\} (\tilde{\mathbf{m}} \wedge \partial_b \tilde{\mathbf{m}})_\mu = 0, \quad (4)$$

where $V(\mathbf{r})$ is Hartree potential

$$V(\mathbf{r}) = \frac{e^2}{\epsilon_0} \int d\mathbf{r}' \frac{\tilde{\rho}(\mathbf{r}')}{|\mathbf{r} - \mathbf{r}'|}, \quad (5)$$

and $\tilde{\rho}$ is the skyrmion charge density corresponding to the minimum energy solution, $\tilde{\mathbf{m}}(\mathbf{r})$. The solutions of Eq. (4) can be classified by the skyrmion charge $Q = \int d\mathbf{r} \rho(\mathbf{r})$. In the absence of Zeeman and Coulomb energies the energy functional is scale invariant and Eq. (4) has a family of known analytic scale invariant solutions.^{31–33} The solutions may be represented by analytic complex-valued polynomials:

$$\tilde{\mathbf{m}}(z) = \left(\frac{4w_1}{|w|^2 + 4}, \frac{4w_2}{|w|^2 + 4}, \frac{|w|^2 - 4}{|w|^2 + 4} \right), \quad (6)$$

where $w = w_1 + iw_2$ is a polynomial in the complex variable $z = (x + iy)/\lambda$ with arbitrary scale λ . The degree of the polynomial w determines the skyrmion charge. These analytic solutions are not valid if the Zeeman and Coulomb terms are included. In the following subsection we briefly explain the numerical methods we use to solve the generalized differential equation for the case of unit charge spin texture.

B. Single skyrmion

In this subsection we concentrate our attention on anti-skyrmions (skyrmions) with unit topological charge, $Q = 1(-1)$. We find a numerical solution to Eq. (4) for an infinite system with the boundary condition that the spin is down at the skyrmion center and up at infinity. It is convenient to choose the origin of coordinates at the center of the skyrmion to take advantage of the circular symmetry of the charge distribution of a single skyrmion. We parametrize the order parameter $\mathbf{m}(\mathbf{r})$ by spherical angles so that

$$\mathbf{m}(\mathbf{r}) = (\sin\theta(\mathbf{r})\cos\phi(\mathbf{r}), \sin\theta(\mathbf{r})\sin\phi(\mathbf{r}), \cos\theta(\mathbf{r})), \quad (7)$$

where $\theta(\mathbf{r})$ and $\phi(\mathbf{r})$ are new field variables. We take advantage of the circular symmetry for the single-skyrmion problem by choosing $\theta(r, \varphi) \equiv \theta(r)$ and $\phi(r, \varphi) \equiv \pm \varphi + \varphi_0$ where φ is the azimuthal angle and φ_0 is a constant. The energy of the skyrmion is independent of φ_0 because of the invariance of the energy functional under global rotation of all spins in the plane about the z axis. Positive and negative signs for φ yield antiskyrmion and skyrmion solutions, respectively. One may show explicitly that the above ansatz and boundary conditions yield unit winding number, $Q = \pm 1$, since the charge density in the circularly symmetric case is given by $\rho(r) = \mp (1/4\pi r) [d/dr \cos\theta(r)]$. It follows that skyrmion and antiskyrmion solutions have the same energy, allowing us to consider skyrmion spin textures only.³⁴ In this case, Eq. (4) reduces to a nonlinear integro-differential equation for $\theta(r)$:

$$\begin{aligned} \rho_s \frac{1}{r} \frac{d}{dr} \left(r \frac{d\theta(r)}{dr} \right) - \rho_s \frac{1}{2r^2} \sin[2\theta(r)] - \frac{t}{2\pi\ell_0^2} \sin\theta(r) \\ + \frac{e^2}{16\pi^2} \frac{\sin\theta(r)}{r} \int dr' \frac{dU(r, r')}{dr} \sin\theta(r') \frac{d\theta(r')}{dr'} = 0. \end{aligned} \quad (8)$$

Here

$$U(r, r') \equiv \frac{4}{|r-r'|} K \left(\frac{(-4rr')}{(r-r')^2} \right), \quad (9)$$

where $K(x)$ is the complete elliptic integral of the first kind continued appropriately to negative values of x . We have solved Eq. (8) for $\theta(r)$ using an iterative approach. At each step in the calculation the integral over r' was evaluated at each r using an approximation for $\theta(r)$. When this integral is fixed, we are left with a two-point boundary value problem [$\theta(r=0) = \pi$ and $\theta(r \rightarrow \infty) = 0$] which can be solved by standard methods. The resulting value of $\theta(r)$ is used to evaluate the integral over r' for the next iteration. We found that this iterative procedure converged rapidly when the iteration was started from one of the analytic solutions obtained neglecting Coulomb and Zeeman energies.

Figure 1 illustrates some of the results obtained from these numerical calculations. We plot the size of the skyrmion (λ), defined by $\theta(\lambda) = \pi/2$, and the number of reversed spins (K), defined by

$$K \equiv \frac{1}{4\pi\ell_0^2} \int d\mathbf{r} [1 - m_z(\mathbf{r})] - \frac{1}{2}, \quad (10)$$

as a function of t . We find that $\lambda \sim t^{-1/3}$ and $K \sim t^{-2/3}$. The logarithmic corrections to these power laws predicted on the basis of a variational solution of the field theory⁶ are not yet apparent at the smallest values of t we have considered.

Figure 2 presents our numerical results for the dependence of skyrmion energy on Zeeman coupling strength in the minimal field theoretical description. The Belavim-Polyakov solutions of Eq. (6) have the minimum possible gradient energy, which has the value $4\pi\rho_s$. When the Zeeman

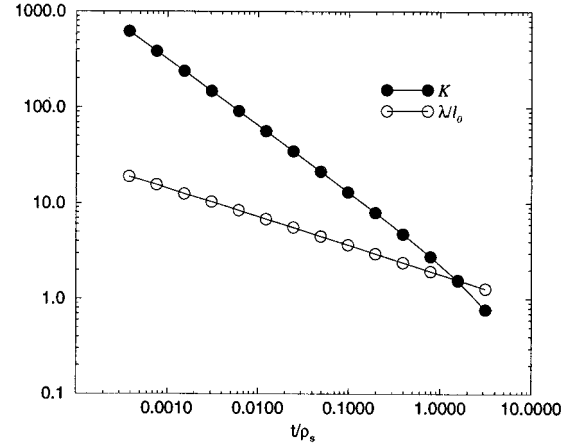


FIG. 1. Skyrmion size (circles) and spin (black dots) obtained from the classical field theory as a function of the Zeeman coupling constant t . The skyrmion size λ is defined as the radius at which the spin lies in the xy plane, i.e., $\cos[\theta(\lambda)] = 0$. These results are consistent with the power law $\propto t^{-1/3}$ behavior expected at small t . The number of reversed spins in a skyrmion is proportional to $\lambda^2 \propto t^{-2/3}$. Its deviation from these power laws at large t is an indication of the necessity for including microscopic physics not captured by the minimal field theory.

man and the Coulomb terms are added the skyrmion texture is reshaped and the optimal solutions are no longer analytic in z . In particular,⁶ the component of the magnetization perpendicular to the Zeeman field has an exponential rather than a logarithmic fall off at large distances. These nonanalytic solutions must have a gradient energy larger than $4\pi\rho_s$, with the deviation from this value decreasing as the Zeeman energy decreases, or, equivalently, as the size of the skyrmion increases. We thus expect that for the gradient energy $E_0(\lambda) = 4\pi\rho_s + f(\lambda)$ where $f(\lambda)$ is a monotonically decreasing function of the skyrmion's size (see Fig. 2). The nonanalytical solutions become asymptotically close to the

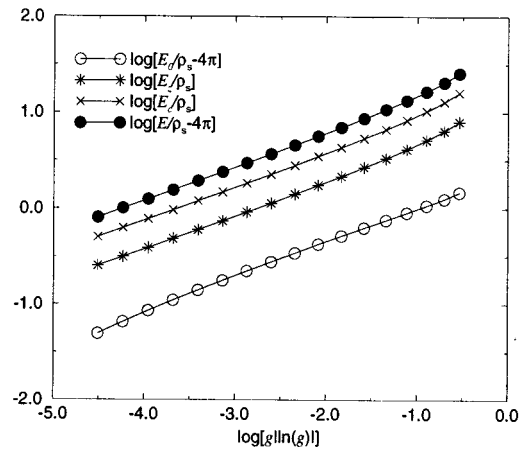


FIG. 2. Skyrmion energies: E_c (crosses), E_z (stars), excess gradient energy $E_0 - 4\pi\rho_s$ (circles), and total excess energy (black dots) as a function of $\log_{10}[g \ln(g)]$ [g is the Zeeman spin splitting in units of $e^2/(\epsilon\ell_0)$]. The power law for the dependence of the excess skyrmion energy, which we extract from a linear fit to these plots, is close to $1/3$.

Belavim-Polyakov solutions at small Zeeman splitting (large λ). Dimensional analysis shows that, up to possible logarithmic factors, the Coulomb and the Zeeman energies must vary at large λ as C/λ and $D\lambda^2$, respectively, where $C \propto e^2/\epsilon$ and $D \propto t/\ell_0^2$ are constants. Assuming that $f(\lambda)$ vanishes faster than $1/\lambda$, optimizing the total energy $[4\pi\rho_s + f(\lambda) + C/\lambda + D\lambda^2]$ with respect to λ leads to the prediction $E_z = E_c/2\alpha(e^2/\epsilon\ell_0)^{2/3}t^{1/3}$ as $\lambda \rightarrow \infty$. These power laws were originally suggested⁶ by Sondhi *et al.* Our numerical results confirm these predictions, which hold with surprising accuracy out to fairly large values of t : in fact E_z/E_c is within 1% of its asymptotic value in the whole range of values of λ we have studied. The fact that $f(\lambda)$ vanishes faster than λ^{-1} is expected on the basis of perturbative treatments of the Coulomb and Zeeman terms and confirmed by the numerical results shown in Fig. 2. The total energy of the skyrmion is closely given by $E/\rho_s = 4\pi + A[g|\ln(g)|]^{1/3}$, where $g = 2t/(e^2/\epsilon\ell_0)$ and, from Fig. 2, we estimate the dimensionless constant $A \approx 30$. (Unlike the results for λ and K , the logarithmic factor in the energy is apparent in our numerical results at small Zeeman coupling strengths.) This numerical estimate of A compares reasonably well with previous estimates^{6,35} in which the result $A \approx 25$ is obtained. The consistency of these numerical results affords confidence in their accuracy.

III. MICROSCOPIC DESCRIPTIONS OF SINGLE-SKYRMION STATES

A. Exact diagonalizations

The microscopic physics of skyrmions can be approached directly by numerically diagonalizing the finite-size Hamiltonian matrix for N two-dimensional spin-1/2 electrons in N_ϕ lowest Landau level orbitals.^{6,36,37} The Hamiltonian commutes with the total spin operator, \hat{S}^2 , and, when the Zeeman term is neglected, also with its projection, \hat{S}_ξ , on any direction ξ . When the Zeeman coupling is present the direction ξ must correspond with the direction of the field. All the eigenstates of the system can be labeled by the quantum numbers S and S_ξ . As mentioned in the Introduction, the particular case $N = N_\phi$ corresponds to $\nu = 1$ and, although there is no rigorous proof, numerical evidence clearly indicates that the ground state has the maximum possible total spin $S = N/2$ and, in the absence of a Zeeman field, a degeneracy $2S + 1$. As pointed out by Jain and Wu,³⁹ this is one of the few cases where the first Hund rule applies in the fractional Hall regime. When the Zeeman field is in the \hat{z} direction, the ground state has $S_z = N/2$ and the electronic system is completely spin polarized in the direction of the field at zero temperature.

Since skyrmions are charged quasiparticles, they appear in exact diagonalization calculations performed with $N = N_\phi \pm 1$. (Particle-hole symmetry permits examination of one sign of charge only.) In order to obtain the energy spectrum in the spherical geometry^{6,36,37} we need all interaction matrix elements in the lowest shell of monopole harmonics³⁸ which comprise the lowest Landau level basis. These are given by

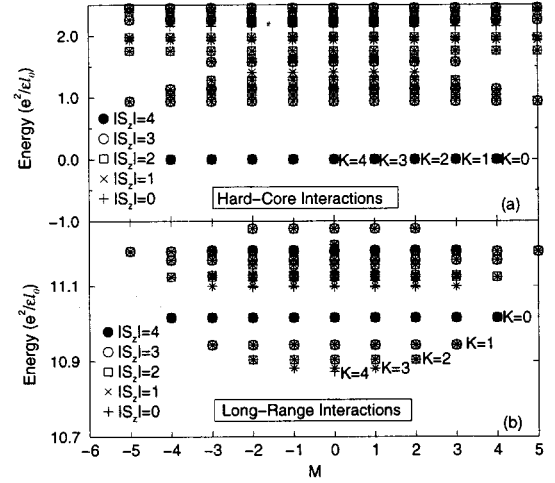


FIG. 3. Energy spectrum obtained from an exact diagonalization of the Hamiltonian in the spherical geometry with $N=8$ and $N_\phi=9$ for (a) hard-core and (b) long-range (Coulomb) interactions (no Zeeman coupling included). Different symbols have been used for different values of $|S_z|$. For the case of the hard-core model a degenerate band corresponding to the Landau level degeneracy occurs once for each member of each $S = N/2 - K$ multiplet present at this system size. For the case of long-range interactions the degeneracy is removed and the energy decreases as $K(S)$ increases (decreases). Rotational symmetry is always present in the spherical geometry and the Landau level degeneracy of the charged quasiparticles is preserved for each value of K .

$$\langle m_1 m_2 | V(\vec{\Omega} - \vec{\Omega}') | m_3 m_4 \rangle = \frac{e^2}{\epsilon\ell_0} (-1)^{m+m_1+m_2} \times \sum_{l=|m|}^{2N_S} \begin{pmatrix} N_S & l & N_S \\ -m_1 & -m & m_4 \end{pmatrix} \times \begin{pmatrix} N_S & l & N_S \\ -m_2 & m & m_3 \end{pmatrix} V_l^{N_S}, \quad (11)$$

where $m = m_4 - m_1 = m_2 - m_3$ and the m_i are the azimuthal angular momentum quantum numbers which label the single-particle orbitals, $V(\vec{\Omega} - \vec{\Omega}')$ is the interaction potential where $\vec{\Omega}$ denotes the electronic spherical coordinate, and $N_S = (N_\phi - 1)/2$. The coefficients in this expansion are products of Wigner's 3- j symbols and the $V_l^{N_S}$ parameters are the interaction-dependent pseudopotentials introduced by Haldane. Since the Hamiltonian also commutes with the total orbital angular momentum \hat{L} the diagonalization is carried out in subspaces of fixed S_z and $M \equiv L_z$. It is instructive to consider first the hard-core model for the electron-electron interactions. In this case the pseudopotentials $V_l^{N_S}$ are given by

$$V_l^{N_S} = \frac{(2N_S + 1)^2 (2l + 1)}{\sqrt{N_S}} \begin{pmatrix} N_S & l & N_S \\ -N_S & 0 & N_S \end{pmatrix}^2. \quad (12)$$

For this model, as illustrated in Fig. 3(a) and discussed previously by Jain and Wu³⁹ and MacDonald, Fertig, and Brey,⁹ multiplets of zero-energy eigenstates occur with all possible values of the total spin quantum number S . In a quantum

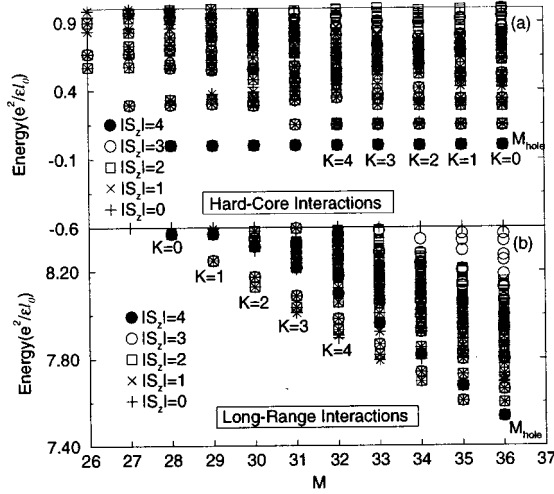


FIG. 4. Energy spectrum obtained from an exact diagonalization of the Hamiltonian for a disk geometry with $N=8$ and $N_\phi=9$, for (a) hard-core and (b) long-range (Coulomb) interactions (no Zeeman coupling included). Different symbols have been used for different values of $|S_z|$. As in Fig. 3 for the case of the hard-core model, a degenerate band at zero energy is observable where all possible values of K are present. Unlike in the spherical geometry for the case of long-range interactions the translational symmetry is broken due to strong edge effects.

description, the number of reversed spins in a skyrmion spin texture is quantized and conjugate⁹ to its global orientation. The zero-energy spin multiplets with $S=N/2-K$ have been shown⁹ to be the quantum states which correspond to a classical skyrmion texture with K reversed spins. The results shown in Fig. 3(b) are for the case of Coulomb interactions between the spins, for which the pseudopotentials are

$$V_l^{N_S} = \frac{(2N_S+1)^2}{\sqrt{N_S}} \begin{pmatrix} N_S & l & N_S \\ -N_S & 0 & N_S \end{pmatrix}. \quad (13)$$

In this case skyrmion states with more reversed spins have lower energy, at least when the Zeeman energy is neglected. When the Zeeman energy is included, the energy will in general be minimized at an intermediate value of K . This is the result obtained by Rezayi,³⁶ which provided evidence for the existence of charged excitations with large spin quantum numbers in quantum Hall ferromagnets. The appearance of degenerate states with different total angular momenta reflects the extensive Landau level degeneracy of single-skyrmion states with all values of K .

We have also performed the same calculation ($N=8$, $N_\phi=9$) in the disk geometry. Figure 4(a) shows the low-energy spectrum for the hard-core model where one can see the same degenerate band at zero energy as in the spherical geometry case. For the zero-energy states of the hard-core model the Landau level degeneracy is preserved. For the Coulomb interaction, on the other hand, Landau level degeneracy is broken by strong edge effects [see Fig. 4(b)] and the nonlocal nature of the interaction. For a given value of M , the minimum interaction energy state is always found at the maximum allowed value of K .

B. Hartree-Fock

A simpler and perhaps physically more transparent microscopic approach for computing skyrmion properties is the unrestricted Hartree-Fock approximation approach. This procedure finds the lowest-energy Slater determinant wave function which supports a spin texture of the form found in skyrmion solutions of the $NL\sigma$ model. Such wave functions generically have the form⁸ (for quasihole skyrmions)

$$|\Psi_{\text{HF}}\rangle = \prod_{m=0}^{\infty} (u_m c_{m\downarrow}^\dagger + v_m c_{m+1\uparrow}^\dagger) |0\rangle, \quad (14)$$

where $c_{m\sigma}^\dagger$ creates a lowest Landau level electron in angular momentum state m with spin σ , and the u_m, v_m 's are variational parameters obeying the constraint $|u_m|^2 + |v_m|^2 = 1$. The precise way in which the energy of the state $|\Psi_{\text{HF}}\rangle$ may be minimized with respect to the u_m, v_m 's has been discussed elsewhere.⁸

In practical calculations, the Hartree-Fock approach bridges the gap between skyrmion sizes which can be reached with exact diagonalization approaches and system sizes where the field theoretic approach becomes accurate. Typically one is limited to system sizes with $N_\phi \approx 10$ in finite-size diagonalization studies, since the matrix dimensions grow rapidly with system size. On the other hand, Hartree-Fock calculations are possible for spin textures involving up to several thousand electrons. As in exact diagonalization studies one works with the exact many-body Hamiltonian in Hartree-Fock studies so that the quantitative errors introduced in the gradient expansion of the energy functional used to generate the $NL\sigma$ model for the quantum Hall ferromagnet⁵⁻⁷ are not present. The Hartree-Fock approach also captures some of the quantum mechanics of the problem, though clearly not all. In particular, $|\Psi_{\text{HF}}\rangle$ has $M - S_z$, the difference of the orbital and the z component of the spin angular momenta, as a good quantum number. However, M and S_z are *not* separately quantized as they should be, nor is $|\Psi_{\text{HF}}\rangle$ an eigenfunction of \hat{S}^2 . These failures could easily have some quantitative importance for $K \sim 3$, the quantum number of the lowest-energy skyrmion in typical experiments. From a field theoretic point of view, one may regard the Hartree-Fock approximation as a mean field theory which retains the higher-order gradient terms absent in the simpler field theory studied in the preceding section. The resulting effective action would contain most information, but, in principle, one should include quantum fluctuations around this stationary phase approximation in order to properly account for the quantization of orbital and spin angular momentum. As shall be seen below, for the purposes of computing energies and sizes of the skyrmions, the Hartree-Fock approach appears to be remarkably accurate, suggesting that such quantum fluctuations are quantitatively unimportant. However, for probes sensitive to the quantum numbers of the skyrmions—tunneling spectroscopy, for example—wave functions with the correct quantum numbers are needed to obtain qualitatively correct results.⁴⁰

C. Variational wave functions

An alternate quantum description of single-skyrmion states can be obtained by using variational many-body wave

functions. These can be refined by comparing with numerically exact solutions for small K and can provide a convenient, if somewhat indirect, route to calculate properties of physical interest $N_\phi \rightarrow \infty$ limit. The variational wave functions we employ are motivated by the disk-geometry wave functions introduced by MacDonald, Fertig, and Brey⁹ which, in the thermodynamic limit, become exact for hard-core-interaction single-skyrmion states. The second quantized form of these wave functions clearly exhibits the microscopic nature of the skyrmion:

$$|\Psi_K^0\rangle = \frac{1}{\sqrt{C(K)}} \sum_{m_K > \dots > m_1 = 1}^{N_\phi} \frac{1}{\sqrt{m_1 \dots m_K}} \times c_{m_K-1\downarrow}^\dagger c_{m_K\uparrow} \dots c_{m_1-1\downarrow}^\dagger c_{m_1\uparrow} c_{0\uparrow} |\Psi\rangle. \quad (15)$$

In the above expression $|\Psi\rangle$ denotes the ferromagnetic $\nu = 1$ state and $C(K)$ are the normalization constants

$$C(K) = \sum_{m_K > \dots > m_1 = 1}^{N_\phi} \frac{1}{m_1 \dots m_K}. \quad (16)$$

This wave function corresponds to a skyrmion with quantum number K located at the origin of the plane with $M_{\max} = M_{\text{hole}} - K$ (M_{hole} corresponds to the total angular momentum with a bare quasihole located at the origin [see Fig. 4(a)]). All other single-skyrmion states with different orbital angular momenta M within a particular zero-energy K band can be obtained by lowering the center-of-mass angular momentum $n = M_{\max} - M$ times:

$$|\Psi_K^n\rangle \propto \left(\sum_{m=0}^{N_\phi} \sqrt{m+1} (c_{m\uparrow}^\dagger c_{m+1\uparrow} + c_{m\downarrow}^\dagger c_{m+1\downarrow}) \right)^n |\Psi_K^0\rangle. \quad (17)$$

In a large system where edges may be neglected, all such states are degenerate. Here we focus only on the states of highest orbital angular momentum, which are centered at the origin.

It is interesting to note that these wave functions are identical to hard-core model Hartree-Fock wave functions [Eq. (14)] projected onto a state of definite S_z .²⁰ [For the hard-core model, the coefficients u_m, v_m in Eq. (14) may be determined analytically.⁹] Thus they presumably improve on the Hartree-Fock wave function in that they include the quantum fluctuations necessary to obtain the quantization of spin. It should also be noted that Eq. (15) is not precisely an eigenstate of \hat{S}^2 , as may be verified by acting on it with the total spin raising operator S^\dagger . This operator should but fails to annihilate the state for any finite-size system. However, it is easily seen that $S^\dagger |\Psi_K^n\rangle \propto C(K)^{-1/2}$, which vanishes in the thermodynamic limit. Thus the relative weight of this wave function outside its appropriate spin multiplet vanishes with increasing system size.¹⁶

We use these variational wave functions to estimate the energies of single-skyrmion states for the case of Coulomb electron-electron interactions. Because of numerical difficulties created by the long range of this interaction it is convenient to introduce the neutral excitation energy defined as follows:

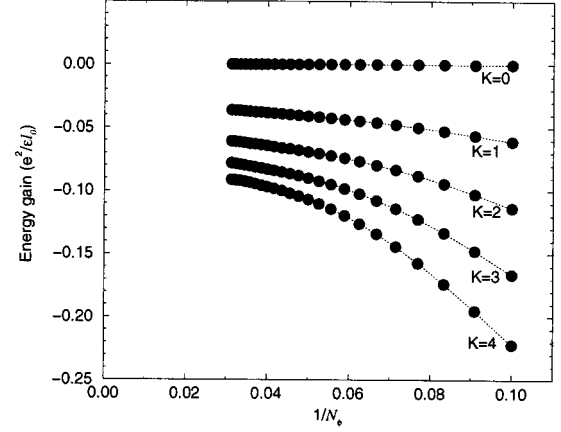


FIG. 5. Energy gain of the skyrmion as a function of $1/N_\phi$ for different values of K . These results were obtained using unmodified hard-core model wave functions in the disk geometry (see text).

$$\epsilon(K) = \epsilon_+(0) + \epsilon_-(K), \quad (18)$$

where $\epsilon_+(0)$ is the energy to make a $K=0$ antiskyrmion (bare spin-reversed electron),

$$\epsilon_+(0) = E(K=0, N=N_\phi+1) - E(N=N_\phi), \quad (19)$$

and $\epsilon_-(K)$ is the energy to make a skyrmion with K reversed spins,

$$\epsilon_-(K) = E(K, N=N_\phi-1) - E(N=N_\phi). \quad (20)$$

The quantity of physical relevance is the difference $\epsilon(K) - \epsilon(0)$, the interaction energy gain resulting from a texture with K reversed spins. The calculation of the neutral excitation energies has been done for up to $N_\phi = 32$ and the results for this energy gain are shown in Fig. 5 as a function of $1/N_\phi$. The edge effects, which bear primary responsibility for the finite-size dependence seen in Fig. 4, are minimized by increasing the angular momentum of the minority-spin electron in the $K=0, N=N_\phi+1$ state in step with K . This allows us to extract reliable results from calculations at fairly small values of N_ϕ .⁴¹ In order to make an accurate extrapolation of these results to the thermodynamic limit we use a Wynn ϵ algorithm to generate Padé approximants.⁴² The results of this extrapolation are shown in Fig. 6, where the same method has been used to extrapolate the exact results obtained in spherical geometry calculations (see Sec. III A) with N_ϕ as large as 11.

The substantial differences between exact diagonalization and variational wave function results is indicative with deficiencies in these wave functions. The source of the difficulty is that these wave functions do not represent a finite-size object as $N_\phi \rightarrow \infty$. [This can be easily seen from the fact that the normalization constants $C(K)$ diverge in the thermodynamic limit.] From coefficients in the expression (15) one can see that the tail in the spin density distribution falls off as $1/r^2$, which coincides with the long-distance behavior of the classical soliton solution in the conventional $\text{NL}\sigma$ model for ferromagnets. However, as stated in Sec. II, the long-distance behavior departs from this form when Coulomb and Zeeman terms are present. In the classical solution the $1/r^2$ behavior

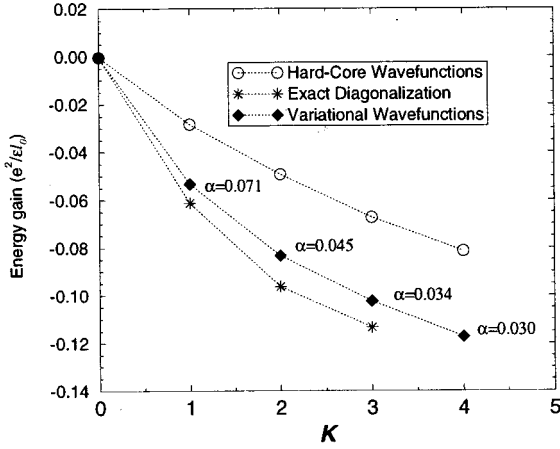


FIG. 6. Energy gain of the skyrmion as a function of K . The plot shows energies obtained using the hard-core wave functions, the optimized variational wave functions, and energies obtained from exact diagonalization in the spherical geometry. We were able to reliably extrapolate the exact diagonalization results only for K up to 3.

is replaced by an exponential decay at large distances. This observation motivates the following refinement in our variational wave functions:

$$|\Psi_K^0(\alpha)\rangle = \frac{1}{\sqrt{A(K)_{m_K}}} \sum_{m_1=1}^{N_\phi} \frac{e^{-\alpha(m_1+\dots+m_K)}}{\sqrt{m_1 \dots m_K}} \times c_{m_K-1\downarrow}^\dagger c_{m_K\uparrow} \dots c_{m_1-1\downarrow}^\dagger c_{m_1\uparrow} c_{0\uparrow} |\Psi\rangle, \quad (21)$$

where the $A(K)$ are the new normalization constants

$$\sum_{m_K > \dots > m_1 = 1}^{N_\phi} \frac{e^{-2\alpha(m_1+\dots+m_K)}}{m_1 \dots m_K}.$$

The parameter α offers the possibility of optimizing the shape of the skyrmion for each value of K .

It is, perhaps, surprising that the introduction of a Coulomb repulsion leads to a more rapid fall off in the reversed spin density at large distances from the skyrmion center. One way of understanding this difference comes from examining the wave functions in Eqs. (15) and (21). For $K=1$ these are sums of products of a quasihole in the $m=0$ orbital and a particle-hole pair with the minority-spin electron precisely one unit of angular momentum lower than majority-spin hole. Since such particle-hole pairs are precisely what are needed to construct spin waves at $\nu=1$,⁴³ it is convenient to think of the state as a spin wave with orbital angular momentum $m=-1$ moving in the presence of a spin-polarized quasihole. For the case of hard-core interactions, it is easy to see that the spin-wave disturbance and the quasihole do not interact. The spin wave is therefore unbound and the linear scale over which the spin disturbance is present is limited only by the system size. For Coulomb interactions, the long-range nature of the interaction leads to quite a different result. Because the spin-minority electron is always closer to the origin than the spin-majority hole, there is an effective *attractive* interaction between the spin wave and the quasihole at the origin. The skyrmion thus represents a state in

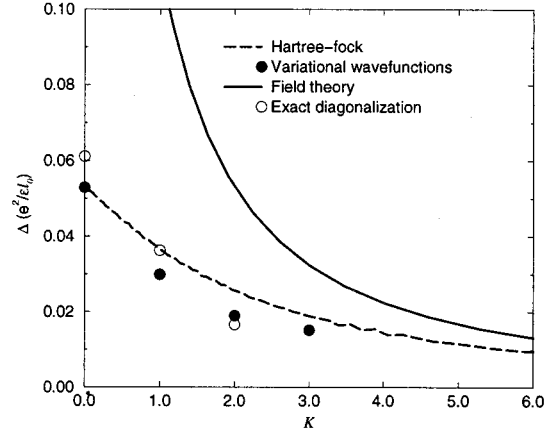


FIG. 7. Skyrmion energy differences $\Delta(K)$ obtained from exact diagonalization (circles), variational wave functions (black dots), the Hartree-Fock approximation (dashed line), and the field theory (solid line). One can see the relative importance of including higher-order gradient contributions (Hartree-Fock) and quantum fluctuations (variational wave functions and exact diagonalizations). $\Delta(K)$ is the Zeeman spin-splitting value at which the number of reversed spins in the lowest-energy skyrmion changes from K to $K+1$.

which the spin wave is bound to the quasihole so that the spin disturbance is localized near the origin. Thus one should expect the weight for large momentum particle-hole pairs to fall off more quickly than for the case of the hard-core interaction. Introduction of the parameter α provides the variational freedom necessary for this to occur.

A deficiency of the states in Eq. (21) is that they are *not* eigenfunctions of \hat{S}^2 (although they are, of course, eigenstates of S_z). They can be modified to have correct quantum numbers at a considerable cost in complexity as discussed in Ref. 40; interested readers are referred to that work for details. The results we obtain using the present wave functions extrapolating to the thermodynamic limit and the values of α that optimize the energies are shown in Fig. 6; the marked improvement over the hard-core interaction wave functions (15) is apparent. As the value of K is increased, the exponential factor becomes irrelevant and one recovers the long-distance behavior expected for classical solitons. This limit has been studied in Ref. 16 and Ref. 15 and the result obtained for the energy of the classical skyrmion⁶ is reproduced by the hard-core wave functions.

IV. COMPARISON

This section is devoted to comparison of results obtained from the classical field theory, Hartree-Fock approximation, and variational wave function for Coulomb interactions between electrons. In Fig. 7 we plot results obtained for $\Delta(K) = \epsilon(K) - \epsilon(K+1)$ calculated with all four approaches. [For the classical field theory and the Hartree-Fock approximation calculations, K is not quantized and we define $\Delta(K) \equiv d\epsilon/dK$.] $\Delta(K)$ is the value of the Zeeman spin-splitting ($2t$ in the notation of this paper) energy at which the single-skyrmion states with K and $K-1$ reversed spins are equal in energy. For GaAs systems $\Delta(K)/(e^2/\epsilon l)$

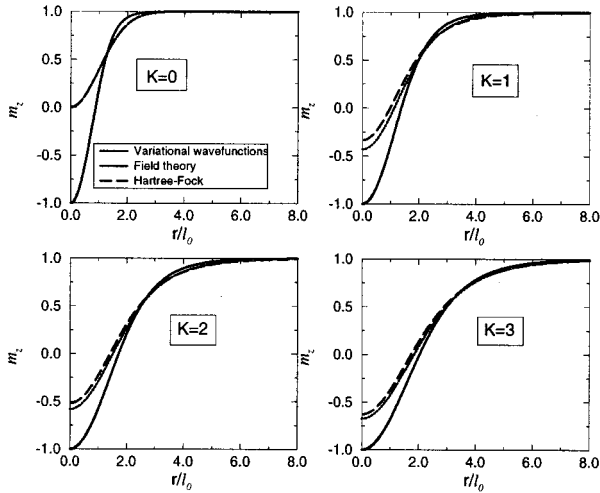


FIG. 8. Radial distribution of m_z in three approximations: classical field theory (solid lines), variational wave functions (dotted lines), and Hartree-Fock (dashed lines). The four smallest spin textures have been considered: $K=0$ (a), $K=1$ (b), $K=2$ (c), and $K=3$ (d). For $K=0$ the results of the variational wave functions and the Hartree-Fock approximation lead to the same solution and, as expected, both schemes converge to the classical field theory for increasing skyrmion size.

$\approx 0.006\sqrt{B[\text{T}]}$, depending somewhat on the details of the semiconductor quantum well so that K is typically ~ 3 for experiments performed at fields ~ 10 T. It is clear from this plot that the corrections to the minimal field theory captured by the Hartree-Fock approximation are sufficient to yield accurate results. The use of leading gradient terms in the minimal field theory is seriously in error for the small K states of practical interest. The additional quantum fluctuation effects included in the variational wave function and exact diagonalization calculations are never of overriding importance.

Figure 8 compares the spin textures by plotting $m_z(r)$ for classical field theory, Hartree-Fock, and variational wave function approaches at small integer values of K . For the classical field theory and Hartree-Fock approximations we plot the solution of Eq. (8), which gives integer values for the number of reversed spins K as defined in Eq. (10). In the quantum calculations

$$m_z(r) = 2\pi \ell_0^2 \sum_m \sum_{s=\pm 1} s n_m^s |\psi_m(\mathbf{r})|^2, \quad (22)$$

where $n_{m\sigma} = \langle \Psi_K^0(\alpha) | c_{m\sigma}^\dagger c_{m\sigma} | \Psi_K^0(\alpha) \rangle$ are single-particle occupation numbers, and $\psi_m(\mathbf{r})$ are the angular momentum states of the lowest Landau level in the symmetric gauge. Note that for the $K=0$ skyrmion state, the variational wave function and the Hartree-Fock calculations are identical. In fact this state is a simple spin-polarized quasihole state which is known to be given exactly by a single Slater determinant. Apparently the fact that the Hartree-Fock approximation becomes exact both for $K=0$ and $K \rightarrow \infty$ leads to good accuracy at all values of K . As expected, the field theory results approach those obtained with the variational wave functions and Hartree-Fock approximations for large enough skyrmions while for small skyrmions there are sig-

nificant differences. The discrepancy is largest for $K=0$ where the classical field theory calculation indicates that the spin is reversed at the origin. In fact this property was one of the boundary conditions used to solve the Euler differential equation of the classical field theory. On the other hand, the quantum calculations show that the z component of the spin is zero at the origin; in fact the total spin density is zero at this point because the total charge density is zero. These changes in the local properties are outside the scope of the generalized $\text{NL}\sigma$ model energy functional. These errors are important for the smallest skyrmions but become less significant with increasing skyrmion size.

On the other hand, the quantum exact diagonalization, variational wave function, and even Hartree-Fock calculations cannot be carried out for very large skyrmions. The limit for the many-body calculations is $K \sim 4$ which is adequate for comparing with existing experiments but not for addressing asymptotic values of various quantities for the very large skyrmions which would be obtained if the Zeeman coupling could be adjusted experimentally to small values. Finite-size effects in these quantum calculations are exacerbated by the long almost algebraic tails of large K skyrmion states. For example, Hartree-Fock calculations with $N_\phi > 1000$ are necessary⁸ to obtain accurate values of $\Delta(K)$ near $K=50$. Similarly it has not proven possible to directly demonstrate the asymptotic behavior, $E \rightarrow 4\pi\rho_s$, as $t \rightarrow 0$ using Hartree-Fock calculations. (However, the asymptotic value may be demonstrated by subtracting the Hartree contribution to the Hartree-Fock energy and noting that this should vanish as the skyrmion size diverges.) For the large skyrmion states, which hopefully will be studied in future experiments, the classical field theoretic approach is accurate and convenient.

The discrepancy between the results of the classical field theory and the microscopic calculations could be reduced by including quantum fluctuations around the classical solution of the minimal field theory. A uniform ferromagnet does not have quantum fluctuations around its fully spin-aligned classical ground state and this is also the exact quantum ground state. However, near a skyrmion center, the spin direction changes with position and quantum fluctuations will occur. As the size of the skyrmion is reduced, these fluctuations will become more important. It is clear that the sign of the effect will be to reduce the spin polarization near the origin and bring the field theory results into closer agreement with the microscopic results. Such calculations have been done for the simple $\text{NL}\sigma$ model.²⁹ However, computation of these fluctuations is numerically difficult,⁴⁴ even at the Gaussian level, in the present model due to the nonlocality of the Coulomb interaction.

V. CONCLUSIONS

We have presented a study of single-skyrmion states of quantum Hall ferromagnets using and comparing a variety of techniques. We have obtained the classical saddle point solution of the appropriate nonlinear σ model modified to include the long-range Coulomb interactions and Zeeman coupling. This minimal classical field theory model includes the leading order gradients necessary to obtain stable skyrmions in the presence of Zeeman coupling. We have developed and

evaluated variational wave functions describing states with the appropriate quantum numbers. Finally, we have performed microscopic numerical exact diagonalization calculations on finite-size systems. These results are compared with results obtained using a Hartree-Fock approximation and reported in earlier work.

Our classical field theory results confirm that the skyrmion size scales as the inverse cube root of the Zeeman energy as expected from the competition between the Zeeman energy and the Coulomb energy and predicted earlier⁶ by Sondhi *et al.* We find that, for skyrmion states with small numbers of reversed spins, the Hartree-Fock results are in excellent agreement with many-body exact diagonalization calculations and with calculations based on variational wave functions motivated by exact zero-energy eigenstates of hard-core model systems. Comparison of these calculations suggests that the minimal classical field theory model is not quantitatively adequate for the size of skyrmion which plays an important role in typical experiments in GaAs quantum well systems. On the other hand, quantum Hartree-Fock calculations are shown to be in excellent agreement with many-

body exact diagonalization and variational wave function approaches. Large skyrmion systems may become experimentally available if the Zeeman coupling strength can be tuned to smaller values, for example, by application of uniaxial stress to semiconductor host of the quantum well, and disorder effects can be controlled. In this case quantum calculations become impractical and the classical field theory approach, possibly supplemented by field theory quantum fluctuation calculations, may be necessary to describe experiments.

ACKNOWLEDGMENTS

The authors are grateful to D. Pfannkuche and L. Belkhir for useful discussions. Work at Indiana University and the University of Kentucky was supported by the National Science Foundation under Grants No. DMR-9416906 and No. DMR 95-03814, respectively. M.A. acknowledges financial support from The Center for Theoretical Physics and Mathematics, Tehran. H.A.F. acknowledges financial support from the Research Corporation.

*Center for Theoretical Physics and Mathematics, P. O. Box 11365-8486, Tehran, Iran and Institute for Studies in Theoretical Physics and Mathematics, P. O. Box 19395-1795, Tehran, Iran.

¹*The Quantum Hall Effect*, 2nd ed., edited by R. E. Prange and S. M. Girvin (Springer, New York, 1990).

²*Quantum Hall Effect: A Perspective*, edited by A. H. MacDonald (Kluwer, Boston, 1989).

³T. Chakraborty and P. Pietiläinen, *The Quantum Hall Effects: Fractional and Integral*, 2nd ed., edited by K. von Klitzing, Springer Series in Solid State Sciences Vol. 85 (Springer-Verlag, Berlin, 1995), and references therein.

⁴*The Quantum Hall Effect*, edited by Michael Stone (World Scientific, Singapore, 1992).

⁵D.-H. Lee and C. L. Kane, Phys. Rev. Lett. **64**, 1313 (1990).

⁶S. L. Sondhi, A. Karlhede, S. A. Kivelson, and E. H. Rezayi, Phys. Rev. B **47**, 16 419 (1993).

⁷K. Moon, H. Mori, Kun Yang, S. M. Girvin, A. H. MacDonald, L. Zheng, D. Yoshioka, and Shou-Cheng Zhang, Phys. Rev. B **51**, 5138 (1995); S. M. Girvin and A. H. MacDonald, in *Novel Quantum Liquids in Semiconductor Structures*, edited by S. Das Sarma and A. Pinczuk (Wiley, New York, 1996).

⁸H. A. Fertig, L. Brey, R. Côté, and A. H. MacDonald, Phys. Rev. B **50**, 11 018 (1994); H. A. Fertig, L. Brey, R. Côté, A. H. MacDonald, A. Karlhede, and S. L. Sondhi, *ibid.* **55**, 10 671 (1997).

⁹A. H. MacDonald, H. A. Fertig, and L. Brey, Phys. Rev. Lett. **76**, 2153 (1996).

¹⁰L. Brey, H. A. Fertig, R. Côté, and A. H. MacDonald, Phys. Rev. Lett. **75**, 2562 (1995).

¹¹S. E. Barrett, G. Dabbagh, L. N. Pfeiffer, K. W. West, and R. Tycko, Phys. Rev. Lett. **74**, 5112 (1995); R. Tycko, S. E. Barrett, G. Dabbagh, L. N. Pfeiffer, and K. W. West, Science **268**, 1460 (1995).

¹²A. Schmeller, J. P. Eisenstein, L. N. Pfeiffer, and K. W. West, Phys. Rev. Lett. **75**, 4290 (1995).

¹³E. H. Aifer, B. B. Goldberg, and D. A. Broido, Phys. Rev. Lett. **76**, 680 (1996).

¹⁴V. Bayot, E. Grivei, S. Melinte, M. B. Santos, and M. Shayegan,

Phys. Rev. Lett. **76**, 4584 (1996); V. Bayot, E. Grivei, J.-M. Beuken, S. Melinte, and M. Shayegan (unpublished).

¹⁵R. K. Kamilla, X. G. Wu, and J. K. Jain, Solid State Commun. **99**, 289 (1996).

¹⁶J. H. Oaknin, L. Martín-Moreno, and C. Tejedor, Phys. Rev. B **54**, 16 850 (1996).

¹⁷A. Karlhede, S. A. Kivelson, K. Lejnell, and S. L. Sondhi, Phys. Rev. Lett. **77**, 2061 (1996).

¹⁸H. A. Fertig, L. Brey, R. Côté, and A. H. MacDonald, Phys. Rev. Lett. **77**, 1572 (1996).

¹⁹Kun Yang and S. L. Sondhi, Phys. Rev. B **54**, 2331 (1996).

²⁰Chetan Nayak and Frank Wilczek, Phys. Rev. Lett. **77**, 4418 (1996).

²¹M. Stone, Phys. Rev. B **53**, 16 573 (1996).

²²Tin-Lun Ho, Phys. Rev. Lett. **73**, 874 (1994).

²³A. G. Green, I. I. Kogan, and A. M. Tselvik, Phys. Rev. B **54**, 16 838 (1996).

²⁴X.-G. Wu and S. L. Sondhi, Phys. Rev. B **51**, 14 725 (1995).

²⁵J. J. Palacios, D. Yoshioka, and A. H. MacDonald, Phys. Rev. B **54**, R2296 (1996).

²⁶A. M. Polyakov, Phys. Lett. **59B**, 79 (1975); J. P. Rodriguez, Phys. Rev. B **39**, 2906 (1989).

²⁷F. D. M. Haldane, Phys. Rev. Lett. **61**, 1029 (1988).

²⁸A. Auerbach, B. E. Larson, and G. N. Murthy, Phys. Rev. B **43**, 11 515 (1991).

²⁹Assa Auerbach, *Interacting Electrons and Quantum Magnetism* (Springer-Verlag, Berlin, 1995).

³⁰Eduardo Fradkin, *Field Theories of Condensed Matter Systems* (Addison-Wesley, Redwood City, 1991).

³¹R. Rajaraman, *Solitons and Instantons* (North-Holland, Amsterdam, 1982).

³²A. A. Belavim and A. M. Polyakov, Pis'ma Zh. Éksp. Teor. Fiz. **22**, 503 (1975) [JETP Lett. **22**, 245 (1975)].

³³G. Woo, J. Math. Phys. (N.Y.) **18**, 1264 (1977).

³⁴This symmetry exists in the field theory description at any value of ν whereas particle-antiparticle symmetry holds in the microscopic theory only at $\nu = 1$.

- ³⁵D. Lilliehöök, K. Lejnell, A. Karlhede, and S. L. Sondhi (unpublished).
- ³⁶E. H. Rezayi, Phys. Rev. B **36**, 5454 (1987); **43**, 5944 (1991).
- ³⁷X. C. Xie and S. He, Phys. Rev. B **53**, 1046 (1996).
- ³⁸T. T. Wu and C. N. Yang, Nucl. Phys. B **107**, 365 (1976); Phys. Rev. D **16**, 1018 (1977).
- ³⁹J. K. Jain and X. G. Wu, Phys. Rev. B **49**, 5085 (1994).
- ⁴⁰J. J. Palacios and H. A. Fertig (unpublished).
- ⁴¹For $K=1$ and $K=2$ one can do the calculation for a sufficiently large number of particles ($N \approx 100$) to eliminate edge effects entirely. Values obtained for the single-skyrmion state energies are similar to those obtained here and support the extrapolation procedures we employ. D. Yoshioka (private communication).
- ⁴²See, for instance, Hiroshi Betsuyaku, Phys. Rev. B **34**, 8125 (1986).
- ⁴³C. Kallin and B. I. Halperin, Phys. Rev. B **30**, 5655 (1984).
- ⁴⁴M. Abolfath and S. M. Girvin (unpublished).